European Scientific Journal May 2013 edition vol.9, No.15 ISSN: 1857 – 7881 (Print) e - ISSN 1857- 7431

ACCURACY ASSESSMENT OF CENTROID COMPUTATION METHODS IN PRECISE GPS COORDINATES TRANSFORMATION PARAMETERS DETERMINATION - A CASE STUDY, GHANA

Yao Yevenyo Ziggah, MSc. Candidate

Hu Youjian, Professor

Christian Amans Odutola, MSc. Candidate

Tien Thanh Nguyen, PhD Candidate

China University of Geosciences, Faculty of Information Engineering, Department of Geodesy and Survey Engineering, Wuhan-Hubei, P.R.China

Abstract

The concept of centroid is significant for many geo-spatial applications especially in the determination of GPS coordinate transformation parameters for transforming coordinates between two geodetic datums. It estimates centroid coordinates system which is in return used in conjunction with the coordinates to estimate the parameters. Choosing an appropriate centroid technique that produces more realistic result is of paramount interest to geospatial professionals. To achieve this, the three-dimensional similarity method known as the Veis transformation model was applied to four different centroid computation procedures to investigate and assess their accuracies and performance in precise GPS datum transformation parameters estimation within Ghana Geodetic Reference Network. In order to ascertain the precision of the derived transformation parameters from the various centroid approaches, the reference standard deviation, reference adjustment variance and the individual standard deviations of the parameters determined were used. Residual analysis using maximum negative, maximum positive, mean error and standard error was done to evaluate the performance of the centroid methods. The test of normality of residuals, deterministic model, correlation coefficient, t-test on the derived transformation parameters, t-test on the correlation coefficient and root mean square error were used to evaluate and check the adequacy of the centroid procedures. The arguments are presented in favour of a more suitable centroid strategies using root mean square (RMS) which was able to give the most

precise GPS datum transformation parameters and resulting coordinate values. Thus, the RMS centroid parameters transformed GPS coordinates to local coordinates at highly significant accuracies than arithmetic mean, harmonic mean and median centroid.

Keywords: Centroid, Global Positioning System, Coordinate System, Datum Transformation Model, Transformation Parameters

Introduction

Geospatial and non-geospatial professionals in their day-to-day activities are challenged with the task of integrating geodetic information based on two different incompatible geodetic datums (Ziggah *et al*., 2013). To solve this, 3D similarity transformation models consisting of three translations, three rotations and one scale factor (Featherstone and Vanicek, 1999; Kutoglu *et al*., 2002) are used to estimate the transformation parameters. Several transformation models have been put forth to compute transformation parameters for geodetic reference network for countries (Thomson, 1994; Hofmann-Wellenhof *et al*., 1997; Constantin-Octavian, 2006; Ayer and Tienhah, 2008) such as Ghana. The most commonly used among these models in Ghana are the conformal similarity methods of Bursa-Wolf, Molodensky-Badekas and Helmert similarity because of their simplicity in application unlike the Veis transformation model.

The Veis transformation model is more complex to apply; but despite these, it usually eliminates correlation existing between the determined parameters which is the case as in Bursa-Wolf model. These correlations are removed as a result of the introduction of centroid coordinate system into the Veis model. Although, there are several techniques available to assist geospatial and non-geospatial professionals in the estimation of transformation parameters, centroid still remains the most basic tool for obtaining reliable information on the translation parameters. Also, the centroid provides the best account for variable scale, survey errors and distortions within the local geodetic network (Ziggah *et al*., 2013). In addition, they give direct measurement of many important properties in transformation model equations in particular, coordinates of the point about which the coordinate reference frame is rotated (OGP, 2012). Many researchers (Kutoglu *et al*., 2002; Newone *et al*., 2003; Marzooqi *et al*., 2005; Constantin-Octavian, 2006; Deakin, 2007; Dzidefo, 2011) in Ghana and around the world applied arithmetic mean centroid method to calculate the centroid coordinate values.

However, several centroid techniques are available for estimating the centroid values for a geodetic network that has not yet been tested. In addition, no assessment of these methods

has been covered in literature, for example, in Ghana to determine the precise method that can give more reliable parameters and resulting coordinate values. In view of the above development, this study seeks to investigate and compare the various centroid techniques for the study area by determining their associated transformation parameters so that users from all related disciplines can utilize them without any problem. It also attempts to come out with an appropriate centroid method that yields the most precise transformation parameters in view of setting a standard in parameter estimation. This study used Veis transformation model which is yet to be applied to the Ghana geodetic reference network (GGRN).

Veis Transformation Model

The execution of the Veis transformation model in this study came with some challenges. For example, Thomson (1994) applied the combined least squares adjustment technique instead of the parametric technique to estimates the parameters likewise in Leick and Gelder (1975) where the similarity based datum-shifts methods were compared. In addition, in Rapp (1993), only the general form of the Veis model equation was stated. However, in this study, the parametric least squares solution approach is considered, therefore it will be prudent to express the Veis transformation model in the least squares parametric terms. The least squares parametric expression of the Veis formula derived in this study follows a similar method Deakin (2006) applied in deriving the Molodensky-Badekas transformation model. Although, the least squares parametric expression of the Veis formula is not readily available in geodesy and surveying textbooks, it surely will exists in associated literature such as technical reports and related articles. Hence, the author makes no claim of originality here. The Veis transformation is defined as (Rapp, 1993):

$$X_v = \vec{T}_v + x_0 + (1+\Delta S_v)M(\varphi_0, \lambda_0, \alpha, \xi, \eta)(x - x_0) \tag{1}$$

This can also be represented as;

$$I_2 = T_2 + G_2 + (1+\Delta S)R_V(\varphi_0, \lambda_0, \varepsilon, \eta)\overline{I_1} \tag{2}$$

Alternatively, equation (2) can be written using vector equations as

$$I_2 = \Delta t_2 + (1+\Delta S)R_V(\varphi_0, \lambda_0, \varepsilon, \eta)\overline{I_1} \tag{3}$$

where R_V is the rotation matrix given as;

$$R_V = \begin{bmatrix} 1 & \alpha\sin\varphi_0 - \eta\cos\varphi_0 & -\alpha\cos\varphi_0\sin\lambda_0 - \xi\cos\lambda_0 - \eta\sin\varphi_0\sin\lambda_0 \\ -\alpha\sin\varphi_0 + \eta\cos\varphi_0 & 1 & \alpha\cos\varphi_0\cos\lambda_0 - \xi\sin\lambda_0 + \eta\sin\varphi_0\cos\lambda_0 \\ \alpha\cos\varphi_0\sin\lambda_0 + \xi\cos\lambda_0 + \eta\sin\varphi_0\sin\lambda_0 & -\alpha\cos\varphi_0\cos\lambda_0 + \xi\sin\lambda_0 - \eta\sin\varphi_0\cos\lambda_0 & 1 \end{bmatrix}$$

$$\bar{I}_1 = \begin{bmatrix} X_{war} - X_G \\ Y_{war} - Y_G \\ Z_{war} - Z_G \end{bmatrix}_1 = \begin{bmatrix} \overline{X} \\ \overline{Y} \\ \overline{Z} \end{bmatrix}_1 \tag{4}$$

X_G, Y_G, Z_G are coordinates of the centroid given as $X_G = \frac{1}{n}\sum_{i=1}^{n} X_i$, $Y_G = \frac{1}{n}\sum_{i=1}^{n} Y_i$, $Z_G = \frac{1}{n}\sum_{i=1}^{n} Z_i$ and (X_i, Y_i, Z_i) are coordinates in the source datum (War Office system).

On the other hand, R_V could be expressed as $R_V = I + U$ (5)

where I is an identity matrix.

$$R_V = \begin{bmatrix} 1 & 0 & 0 \\ 0 & 1 & 0 \\ 0 & 0 & 1 \end{bmatrix} + \begin{bmatrix} 0 & \alpha\sin\varphi_0 - \eta\cos\varphi_0 & -\alpha\cos\varphi_0\sin\lambda_0 - \xi\cos\lambda_0 - \eta\sin\varphi_0\sin\lambda_0 \\ -\alpha\sin\varphi_0 + \eta\cos\varphi_0 & 0 & \alpha\cos\varphi_0\cos\lambda_0 - \xi\sin\lambda_0 + \eta\sin\varphi_0\cos\lambda_0 \\ \alpha\cos\varphi_0\sin\lambda_0 + \xi\cos\lambda_0 + \eta\sin\varphi_0\sin\lambda_0 & -\alpha\cos\varphi_0\cos\lambda_0 + \xi\sin\lambda_0 - \eta\sin\varphi_0\cos\lambda_0 & 0 \end{bmatrix}$$

Hence, (6)

Using equations (4), (5) and substituting into equation (3), the Veis formula can be written as

$$I_2 = (1 + \Delta S)(I + U)\bar{I}_1 + t_2 \tag{7}$$

where $I_2 = [X, Y, Z]_2^T$ are the coordinates in the target datum (WGS 84), $\bar{I}_1 = [\overline{X}, \overline{Y}, \overline{Z}]_1^T$ are the coordinates in the source datum (War Office), t_2 is the vector of translation and ΔS is the scale. Expanding equation (7) gives

$$I_2 = (I + U)\bar{I}_1 + \Delta S(I + U)\bar{I}_1 + t_2$$

$$I_2 = (I + U)\bar{I}_1 + \Delta S I\bar{I}_1 + \Delta S U\bar{I}_1 + t_2 \tag{8}$$

In view of the fact that $R_V = I + U$ and a vector pre-multiplied by the identity matrix is equal to the vector (that is $\Delta S I\bar{I}_1 = \Delta S\bar{I}_1$) and $\Delta S U\bar{I}_1 \approx 0$ because ΔS is small (usually <1ppm) and the off-diagonal elements of U (the small rotations R_X, R_Y, R_Z are usually less

than 1 second arc ($\approx 4.8E-06$), the products will be exceedingly small and may be neglected. Hence, for practical purposes, equation (8) may be written as

$$I_2 = R_V \bar{I}_1 + \Delta S \bar{I}_1 + t_2 \tag{9}$$

Substituting the variable terms in equation (9) for a single control point is given as

$$\begin{bmatrix} X \\ Y \\ Z \end{bmatrix}_2 = \begin{bmatrix} 1 & \alpha \sin\varphi_0 & -\alpha \cos\varphi_0 \sin\lambda_0 \\ & -\eta \cos\varphi_0 & -\xi \cos\lambda_0 \\ & & -\eta \sin\varphi_0 \sin\lambda_0 \\ -\alpha \sin\varphi_0 + \eta \cos\varphi_0 & 1 & \alpha \cos\varphi_0 \cos\lambda_0 \\ & & -\xi \sin\lambda_0 \\ & & +\eta \sin\varphi_0 \cos\lambda_0 \\ \alpha \cos\varphi_0 \sin\lambda_0 & -\alpha \cos\varphi_0 \cos\lambda_0 & \\ +\xi \cos\lambda_0 & +\xi \sin\lambda_0 & 1 \\ +\eta \sin\varphi_0 \sin\lambda_0 & -\eta \sin\varphi_0 \cos\lambda_0 & \end{bmatrix} \begin{bmatrix} \bar{X} \\ \bar{Y} \\ \bar{Z} \end{bmatrix}_1 + \Delta S \begin{bmatrix} \bar{X} \\ \bar{Y} \\ \bar{Z} \end{bmatrix}_1 + \begin{bmatrix} t_X \\ t_Y \\ t_Z \end{bmatrix}_2 \tag{10}$$

Expanding equation (10) gives

$$\begin{bmatrix} X \\ Y \\ Z \end{bmatrix}_2 = \begin{bmatrix} \bar{X}_1 + \bar{Y}_1(\alpha \sin\varphi_0 - \eta \cos\varphi_0) + \bar{Z}_1(-\alpha \cos\varphi_0 \sin\lambda_0 - \varepsilon \cos\lambda_0 - \eta \sin\varphi_0 \sin\lambda_0) \\ \bar{X}_1(-\alpha \sin\varphi_0 + \eta \cos\varphi_0) + \bar{Y}_1 + \bar{Z}_1(\alpha \cos\varphi_0 \cos\lambda_0 - \varepsilon \sin\lambda_0 + \eta \sin\varphi_0 \cos\lambda_0) \\ \bar{X}_1(\alpha \cos\varphi_0 \sin\lambda_0 + \varepsilon \cos\lambda_0 + \eta \sin\varphi_0 \sin\lambda_0) + \bar{Y}_1(-\alpha \cos\varphi_0 \cos\lambda_0 + \varepsilon \sin\lambda_0 - \eta \sin\varphi_0 \cos\lambda_0) + \bar{Z}_1 \end{bmatrix} + \begin{bmatrix} \bar{X}_1 \Delta S \\ \bar{Y}_1 \Delta S \\ \bar{Z}_1 \Delta S \end{bmatrix} + \begin{bmatrix} t_X \\ t_Y \\ t_Z \end{bmatrix} \tag{11}$$

Expanding equation (11) becomes

$$X_2 = \bar{X}_1 + \bar{Y}_1 \alpha \sin\varphi_0 - \bar{Y}_1 \eta \cos\varphi_0 - \bar{Z}_1 \alpha \cos\varphi_0 \sin\lambda_0 - \bar{Z}_1 \varepsilon \cos\lambda_0 - \bar{Z}_1 \eta \sin\varphi_0 \sin\lambda_0 + \bar{X}_1 \Delta S + t_X$$

$$Y_2 = -\bar{X}_1 \alpha \sin\varphi_0 + \bar{X}_1 \eta \cos\varphi_0 + \bar{Y}_1 + \bar{Z}_1 \alpha \cos\varphi_0 \cos\lambda_0 - \bar{Z}_1 \varepsilon \sin\lambda_0 + \bar{Z}_1 \eta \sin\varphi_0 \cos\lambda_0 + \bar{Y}_1 \Delta S + t_Y$$

$$Z_2 = \bar{X}_1 \alpha \cos\varphi_0 \sin\lambda_0 + \bar{X}_1 \varepsilon \cos\lambda_0 + \bar{X}_1 \eta \sin\varphi_0 \sin\lambda_0 - \bar{Y}_1 \alpha \cos\varphi_0 \cos\lambda_0 + \bar{Y}_1 \varepsilon \sin\lambda_0 - \bar{Y}_1 \eta \sin\varphi_0 \cos\lambda_0 + \bar{Z}_1 + \bar{Z}_1 \Delta S + t_Z$$

Expressed as three separate equations gives equation (12) below

$$t_X + \alpha(\bar{Y}_1 \sin\varphi_0 - \bar{Z}_1 \cos\varphi_0 \sin\lambda_0) + \varepsilon(-\bar{Z}_1 \cos\lambda_0) + \eta(-\bar{Y}_1 \cos\varphi_0 - \bar{Z}_1 \sin\varphi_0 \sin\lambda_0) + \bar{X}_1 \Delta S = X_2 - \bar{X}_1$$

$$t_Y + \alpha(-\bar{X}_1 \sin\varphi_0 + \bar{Z}_1 \cos\varphi_0 \cos\lambda_0) + \varepsilon(-\bar{Z}_1 \sin\lambda_0) + \eta(\bar{X}_1 \cos\varphi_0 + \bar{Z}_1 \sin\varphi_0 \cos\lambda_0) + \bar{Y}_1 \Delta S = Y_2 - \bar{Y}_1$$

$$t_Z + \alpha(\bar{X}_1 \cos\varphi_0 \sin\lambda_0 - \bar{Y}_1 \cos\varphi_0 \cos\lambda_0) + \varepsilon(\bar{X}_1 \cos\lambda_0 + \bar{Y}_1 \sin\lambda_0) + \eta(\bar{X}_1 \sin\varphi_0 \sin\lambda_0 - \bar{Y}_1 \sin\varphi_0 \cos\lambda_0) + \bar{Z}_1 \Delta S = Z_2 - \bar{Z}_1$$

Moreover, these equations may be rewritten into another expanded matrix equation for a single control points as

$$\begin{bmatrix} 1 & 0 & 0 & \overline{Y}_1\sin\varphi_0 - \overline{Z}_1\cos\varphi_0\sin\lambda_0 & \overline{Z}_1\cos\lambda_0 & -\overline{Y}_1\cos\varphi_0 - \overline{Z}_1\sin\varphi_0\sin\lambda_0 & \overline{X}_1 \\ 0 & 1 & 0 & -\overline{X}_1\sin\varphi_0 + \overline{Z}_1\cos\varphi_0\cos\lambda_0 & -\overline{Z}_1\sin\lambda_0 & \overline{X}_1\cos\varphi_0 + \overline{Z}_1\sin\varphi_0\cos\lambda_0 & \overline{Y}_1 \\ 0 & 0 & 1 & \overline{X}_1\cos\varphi_0\sin\lambda_0 - \overline{Y}_1\cos\varphi_0\cos\lambda_0 & \overline{X}_1\cos\lambda_0 + \overline{Y}_1\sin\lambda_0 & \overline{X}_1\sin\varphi_0\sin\lambda_0 - \overline{Y}_1\sin\varphi_0\cos\lambda_0 & \overline{Z}_1 \end{bmatrix} \begin{bmatrix} t_X \\ t_Y \\ t_Z \\ \alpha \\ \varepsilon \\ \eta \\ \Delta S \end{bmatrix} = \begin{bmatrix} X_2 - \overline{X}_1 \\ Y_2 - \overline{Y}_1 \\ Z_2 - \overline{Z}_1 \end{bmatrix}$$

The above equation can be represented in the form of $V + BX = f$ as illustrated below.

$$\begin{bmatrix} V_X \\ V_Y \\ V_Z \end{bmatrix} + \begin{bmatrix} 1 & 0 & 0 & \overline{Y}_1\sin\varphi_0 - \overline{Z}_1\cos\varphi_0\sin\lambda_0 & \overline{Z}_1\cos\lambda_0 & -\overline{Y}_1\cos\varphi_0 - \overline{Z}_1\sin\varphi_0\sin\lambda_0 & \overline{X}_1 \\ 0 & 1 & 0 & -\overline{X}_1\sin\varphi_0 + \overline{Z}_1\cos\varphi_0\cos\lambda_0 & -\overline{Z}_1\sin\lambda_0 & \overline{X}_1\cos\varphi_0 + \overline{Z}_1\sin\varphi_0\cos\lambda_0 & \overline{Y}_1 \\ 0 & 0 & 1 & \overline{X}_1\cos\varphi_0\sin\lambda_0 - \overline{Y}_1\cos\varphi_0\cos\lambda_0 & \overline{X}_1\cos\lambda_0 + \overline{Y}_1\sin\lambda_0 & \overline{X}_1\sin\varphi_0\sin\lambda_0 - \overline{Y}_1\sin\varphi_0\cos\lambda_0 & \overline{Z}_1 \end{bmatrix} \begin{bmatrix} t_X \\ t_Y \\ t_Z \\ \alpha \\ \varepsilon \\ \eta \\ \Delta S \end{bmatrix} = \begin{bmatrix} X_2 - \overline{X}_1 \\ Y_2 - \overline{Y}_1 \\ Z_2 - \overline{Z}_1 \end{bmatrix}$$

where;

$$B = \begin{bmatrix} 1 & 0 & 0 & \overline{Y}_1\sin\varphi_0 - \overline{Z}_1\cos\varphi_0\sin\lambda_0 & \overline{Z}_1\cos\lambda_0 & -\overline{Y}_1\cos\varphi_0 - \overline{Z}_1\sin\varphi_0\sin\lambda_0 & \overline{X}_1 \\ 0 & 1 & 0 & -\overline{X}_1\sin\varphi_0 + \overline{Z}_1\cos\varphi_0\cos\lambda_0 & -\overline{Z}_1\sin\lambda_0 & \overline{X}_1\cos\varphi_0 + \overline{Z}_1\sin\varphi_0\cos\lambda_0 & \overline{Y}_1 \\ 0 & 0 & 1 & \overline{X}_1\cos\varphi_0\sin\lambda_0 - \overline{Y}_1\cos\varphi_0\cos\lambda_0 & \overline{X}_1\cos\lambda_0 + \overline{Y}_1\sin\lambda_0 & \overline{X}_1\sin\varphi_0\sin\lambda_0 - \overline{Y}_1\sin\varphi_0\cos\lambda_0 & \overline{Z}_1 \end{bmatrix}$$

$$f = \begin{bmatrix} X_{WGS84} - \overline{X}_1 \\ Y_{WGS84} - \overline{Y}_1 \\ Z_{WGS84} - \overline{Z}_1 \end{bmatrix},\ V = \begin{bmatrix} V_{X_1} \\ V_{Y_1} \\ V_{Z_1} \end{bmatrix},\ \begin{bmatrix} \overline{X} \\ \overline{Y} \\ \overline{Z} \end{bmatrix} = \begin{bmatrix} X_{war} - X_G \\ Y_{war} - Y_G \\ Z_{war} - Z_G \end{bmatrix}$$

To compute the transformation parameters for each of the centroidal methods, the equation $X = (B^T B)^{-1}(B^T f)$ was applied to get the least squares solution. The residuals from the observation equations were calculated using *V=f-BX*.

Centroid Coordinate Computation Methods

The centroid computational methodologies (Deakin, 2007) exploited in this study are elaborated below.

Arithmetic Mean Centroid

$$\overline{X} = \frac{\sum_{k=1}^{n} X_k}{n}, \overline{Y} = \frac{\sum_{k=1}^{n} Y_k}{n} \text{ and } \overline{Z} = \frac{\sum_{k=1}^{n} Z_k}{n}$$

The Harmonic Mean Centroid

$$\frac{1}{\overline{\overline{X}}} = \frac{\sum_{k=1}^{n} \frac{1}{\overline{\overline{X}}_k}}{n}, \frac{1}{\overline{\overline{Y}}} = \frac{\sum_{k=1}^{n} \frac{1}{\overline{\overline{Y}}_k}}{n} \text{ and } \frac{1}{\overline{\overline{Z}}} = \frac{\sum_{k=1}^{n} \frac{1}{\overline{\overline{Z}}_k}}{n}$$

The Median Centroid

If the X, Y and Z coordinates of the *n* points in the local geodetic network are each ordered, from smallest to largest into three arrays $X=[X_1\ X_2\ X_3\ \ldots X_n]$, $Y=[Y_1\ Y_2\ Y_3\ \ldots Y_n]$, $Z=[Z_1\ Z_2\ Z_3\ Z_n]$ then the Median centroid is

For n odd: $\overline{X} = X_k$, $\overline{Y} = Y_k$ and $\overline{Z} = Z_k$ where $K = \frac{n+1}{2}$ and

For n even: $\overline{X} = \frac{X_k + X_{k+1}}{2}, \overline{Y} = \frac{Y_K + Y_{K+1}}{2}$ and $\overline{Z} = \frac{Z_k + Z_{k+1}}{2}$ where $k = \frac{n}{2}$

Root Mean Square Centroid

$$\overline{X} = \sqrt{\frac{\sum_{k=1}^{n} X_k^2}{n}}, \overline{Y} = \sqrt{\frac{\sum_{k=1}^{n} Y_k^2}{n}} \text{ and } \overline{Z} = \sqrt{\frac{\sum_{k=1}^{n} Z_k^2}{n}}$$

Where $\left(\overline{X}, \overline{Y}, \overline{Z}\right)$ are the centroid coordinate values for each methodology described above.

Materials and Methods

Study Area

Ghana is located in West Africa and is bordered by Cote D'Ivoire to the West, Togo to the East, Burkina Faso to the North and the Gulf of Guinea to the South. The country spans an area of 239,460 sq. km with the land mass generally consisting of low plains with a dissected plateau in the south-central area and scattered areas of high relief (Baabereyir, 2009). Lying just above the equator, Ghana has a tropical climate with mean annual temperature ranging between 26ºC and 29ºC but temperature are generally higher in the North than in the South (Baabereyir, 2009). Ghana lies between latitudes 4^0 and 12^0 N and longitude 4^0 E and 2^0 W (Anon, 2013). The country is divided into ten administrative regions as shown in figure 1 below.

Figure 1: Map of Ghana showing the study area (Anon, 2013)

This study covers five out of the ten administrative regions in Ghana. That is; Ashanti, Greater Accra, Western, Central and Eastern (figure 1). These regions form the first phase of

the new established geodetic reference network referred as the Golden Triangle. The Golden Triangle of Ghana has the three largest cities and covers a little over a third of the country with 58% of the total population (Poku-Gyamfi and Schueler, 2008). These regions have almost all the natural resources such as gold, bauxite, manganese, oil, timber and many others found in the country and thus, are of high economic importance. Three permanently operating reference stations have been established at the vertices of this Triangle with eighteen-second order reference stations spatially well distributed in the area in question (Poku-Gyamfi and Schueler, 2008).

Materials

Primary data of geodetic coordinates for both WGS 84 and War Office ellipsoid within GGRN were collected from the Ghana Survey Department sourced from a recent study by Dzidefo (2011). Computer programming codes in Matlab (2012b) were written to handle the parameter estimation for the various centroidal computational methods applied to the Veis transformation model. Plotted control points, data structures, descriptive and summary statistics for the entire study were also produced using Matlab (2012b), Microsoft Excel 2013, and SPSS (Version 20).

Methods

Curvilinear geodetic coordinates of common points in both the WGS 84 and War Office system were first converted into rectangular cartesian coordinate (X, Y, Z). To accomplish this task, the following relationships were applied;

$$X = \frac{a\cos\phi\cos\lambda}{[1-f(2-f)\sin^2\phi]^{1/2}} + h\cos\phi\cos\lambda$$

$$Y = \frac{a\cos\phi\sin\lambda}{[1-f(2-f)\sin^2\phi]^{1/2}} + h\cos\phi\sin\lambda$$

$$Z = \frac{a(1-f)^2\sin\phi}{[1-f(2-f)\sin^2\phi]^{1/2}} + h\sin\phi$$

(13)

Where;

h = ellipsoidal height

a = semi major axis of the reference ellipsoid

f = flattening which measures the differences between the two axes of an ellipsoid.

(ϕ, λ) = geodetic latitude and geodetic longitude

The ellipsoidal parameters used in equation (13) for WGS 84 are; semi-major axis value of 6378137.0 m and a flattening of 1/298. The War Office on the other hand has a semi-major axis value of 6378299.99899 m and a flattening of 1/296. Equation (13) was applied directly

to the WGS 84 curvilinear geodetic coordinates (ϕ, λ, h) to obtain its related rectangular cartesian coordinates $(X, Y, Z)_{WGS84}$. However, equation (13) cannot be readily applied directly for deriving the rectangular cartesian coordinate for the War Office ellipsoidal system. This is because data in the War Office ellipsoid expressed as (ϕ, λ, H) contains only orthometric height. Hence, the applicability of equation (13) is limited in this scenario.

In view of this development, the iterative abridged Molodensky transformation model equation (Deakin, 2004) was first applied to the War Office data (ϕ, λ, H) to determine the approximate (change) difference in ellipsoidal height, Δh. This was then used to estimate h for the War Office using $h_{war} = h_{WGS84} - \Delta h$. Having derived the war office ellipsoidal height, equation (13) was then applied to calculate the rectangular cartesian coordinates for the War Office datum. Hence, there exist common points of all coordinates in both systems at this stage. The centroid computational methods were then applied to estimate their respective centroid values in the War Office system. The Veis transformation model was then executed on the cartesian coordinates of common points in both systems to determine the sets of transformation parameters for each centroid methods. These parameters were estimated via parametric least square adjustment technique expressed mathematically as

$$V + BX = f \quad (14)$$

Where:

V = the vector of residuals

B = the design matrix

X = the vector of parameter estimates and

$\boldsymbol{f}$ = the vector of observations.

In all, nineteen control stations tied to both reference systems within the geodetic reference network were used for the parameter estimation. Finally, statistical analysis was carried out on all parameters determined by each of the four centroid techniques.

Results and Discussion

Centroidal Computational Methods Applied

The centroid methods computed parameters and their corresponding statistic values for transforming War Office data to WGS84 system using Veis transformation model are shown in table 1 below.

Table 1: Summary of the derived Parameters

Parameter	3D Similarity Conformal Method: Veis Transformation Model				
	Arithmetic Mean Centroid	**Harmonic Mean Centroid**	**Median Centroid**	**Root Mean Square Centroid**	**Unit**
t_X	-196.61977±0.1360	-196.60639±0.1872	-196.61725±0.1394	-196.52286±0.7559	M
t_Y	33.36126±0.1360	32.98118±0.1588	33.45488±0.1384	31.35971±0.4637	M
t_Z	322.34385±0.1360	322.27239±0.1592	322.26707±0.1385	321.72989±0.4687	M
α	0.44411±1.5848E-06	0.44379±1.5847E-06	0.44411±1.58E-06	0.44196±1.58E-06	Seconds
ε	-0.03304±2.6477E-06	-0.04140±2.64661E-06	-0.03304±2.65E-06	-0.07754±2.64E-06	seconds
η	-0.00535±2.6548E-06	-0.00855±2.6561E-06	-0.00535±2.65E-06	-0.02283±2.66E-06	Seconds
S	-7.16775±1.5827E-06	-7.16806±1.58272E-06	-7.16759±1.58E-06	-7.16963±1.58E-06	Ppm
Reference SD	0.59298	0.59298	0.59299	0.59293	M
Reference AV	0.35163	0.35162	0.35163	0.35156	M

It is evident from table 1 that the two origins of the reference ellipsoids have a negative displacement on the X-axes and positive displacement on the Y and Z-axes. The translation parameter t_X revealing the existence of a negative displacement from the geocenter suggests that both X-axes in the two reference ellipsoids are moving in opposite directions. Conversely, t_Y and t_Z translation parameters from the geocenter evident from table 1 above show that the axes of both reference ellipsoids move in the same direction.

The reference SD and reference AV from table 1 above represent the reference standard deviation and reference adjustment variance. A Visual observation of table 1 presents a negative scale factor values for arithmetic mean centroid, harmonic mean centroid, median centroid and root mean square centroid. These negative scale factors denote that the geometric shapes of the Ghana War Office and WGS 84 system are reduced when the scale factor is applied in conjunction with the derived parameters for transforming coordinates from War Office to WGS 84 datum and vice versa. Therefore, this further corroborates that, similarity transformation methods such as Veis model preserves shapes and angles but the lengths of lines and the position of points may change.

To have an indication on the precision of the transformation to know how well the transformed coordinates from War Office system agree with the known coordinates in the

WGS84 system, the reference standard deviation for the entire observation and the individual standard deviations for the computed parameters were estimated as shown in table 1 above. The general results in table 1 above relatively show smaller standard deviation values for each centroid method parameters determined, thus, warrant its acceptance. The statistical results also indicated that there is 68% probability that the observation and its associated parameters lie between plus or minus the reference standard deviation from their estimated values in table 1 above. In addition, these standard deviation values obtained will indicate a steep bell-shape on the normal distribution curve.

It is worth mentioning that, the introduction of the centroid coordinate into the Veis transformation model for the War Office datum tends to eliminate the correlation of transformation parameters that exist for example, in Bursa-Wolf model and Helmert similarity method. The centroid coordinates in $\left(\overline{X},\overline{Y},\overline{Z}\right)$ used in the derivation of the parameters are shown in table 2 below.

Table 2: War Office Centroidal Coordinate System Results for Ghana Geodetic Reference Network

CENTROID COMPUTATIONAL METHOD	**ESTIMATED CENTROID COORDINATE VALUES**		
	$\overline{X}$	$\overline{Y}$	$\overline{Z}$
Arithmetic Mean	6339126.395702310	-133380.2930677430	689482.7337759430
Harmonic Mean	6339118.28859574	-81957.5710755134	684112.346309607
Median	6338649.78349864	-142417.481296802	702901.323213948
Root Mean Square	6339130.44886187	146570.120445620	692120.3051639080

Residual Analysis from the derivation of the parameters

The evaluation of the performance of the centroid computational methods applied to the Veis transformation model was focused on the residuals (V_X, V_Y, V_Z) generated in estimating their respective transformation parameters. Figures 2, 3, 4 and 5 below, show the variation of residuals with respect to the observations (control points) when the Veis transformation model was executed in determining the centroid methods associated transformation parameters. In addition, the graphs below also show how much the X, Y and Z coordinates fluctuate along the ideal threshold value of zero on the vertical axes. This threshold value also known as the 90-degree line gives a better indication of the inconsistencies in the models by way of errors in the coordinates

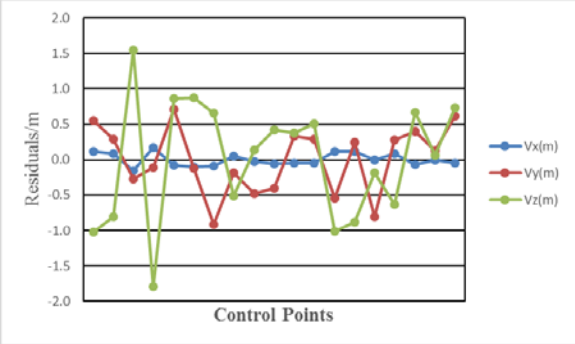

Figure 2: A graph of residuals against the control points for Arithmetic Mean Centroid

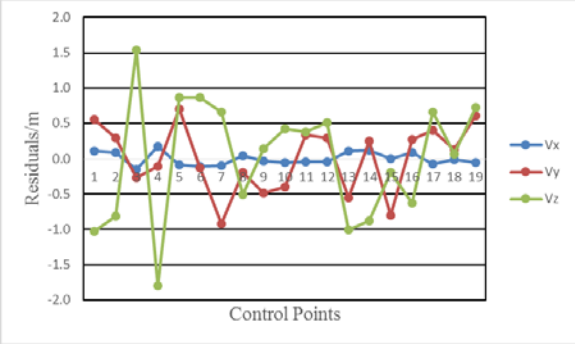

Figure 3: A graph of residuals against the control points for Harmonic Mean Centroid

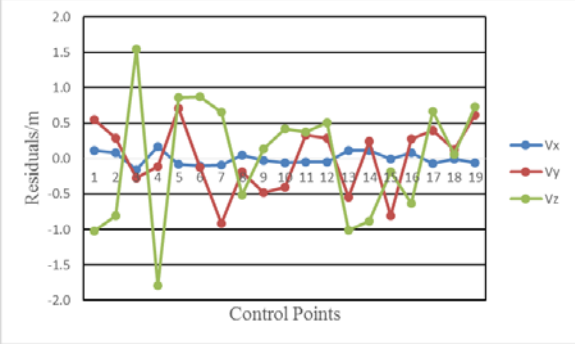

Figure 4: A graph of residuals against the control points for Median Centroid

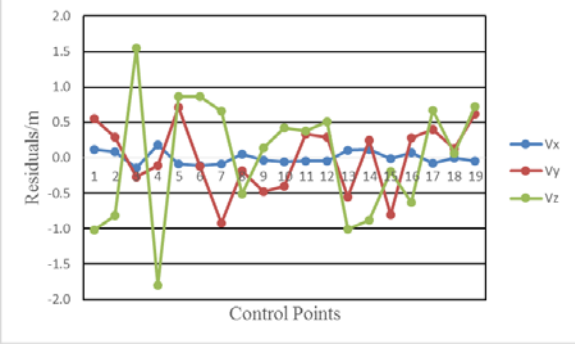

Figure 5: A graph of residuals against the control points for Root Mean Square Centroid

A careful observation in figures 2, 3, 4 and 5 above reveal a large V_Z in the centroid computational methods compared to the V_Y and V_X where there is a graphical evidence of improvement in the horizontal fluctuation along the threshold. Comparatively, the residuals in the horizontal positions of the centroid methods show a fairly consistent rise and fall

around the threshold. Nonetheless, based on visual observation of the graphs of figures 2, 3, 4 and 5, it was seen that, in the V_Z component, there was a significant rise from control point 2 (CFP 200) to point 3 (CFP 225), a downward fall from control point 3 (CFP 225) to point 4 (GCS 102) and another sharp increase from control point 4 (GCS 102) to point 5 (CFP 155) respectively. In the case of the V_X, the residuals are relatively smaller and closer to the displacement threshold value than the V_Y residuals which have a steady rise and fall. These inconsistencies incurred as explained above during the parameter determination can be attributed to three factors. Firstly, is due to the distortions in scale and orientation existing in the old datum (War Office) which could not be absorbed and modeled completely by the Veis transformation model. Secondly, the possible non-parallelism existing between the axes of the coordinate systems of WGS 84 and War Office datum. Finally, the random errors existing in both observation data applied in the parameter determination have an influence on the outcome of the estimation even though this depends on the confidence interval. These factors however, have contributed to the inability of the Veis transformation model to notice its potential of providing higher (sub-meter or even sub-centimeter) accuracy even though it is a rigorous model.

The observational residuals obtained from each centroid approach can be statistically tested and the better method can be chosen. It is therefore, imperative to determine whether the residuals are normally distributed before any statistical test can be carried out. However, if the residuals are not normally distributed then the results obtained may be biased by systematic errors. Hence, to test the normality assumptions of the residuals, normality probability plots for all the centroidal methodologies were carried out. A sample of the normality probability plots of the residuals carried out for each centroid method is shown in figure 6 below.

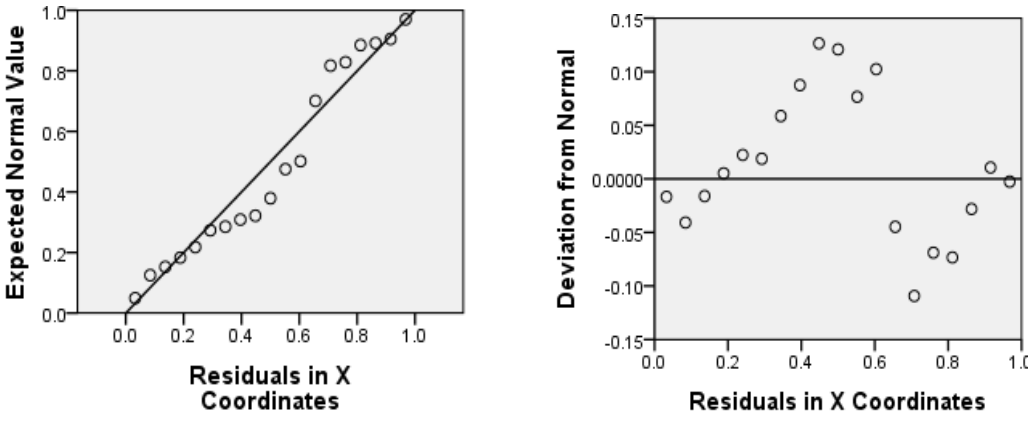

(a) Normality P-P Plots (b) Detrended Normal P-P Plot

Figure 6: Arithmetic Mean Centroid Normality Probability Plots

As shown in figure 6 (a) above, the data appear to constantly spread along the 45-degree line which further confirms that the observation conforms to the expected normal and the assumption of normally distributed error is met. In the detrended version, figure 6 (b), the pattern of points above and below the horizontal zero line is random. This was observed for all the four centroid methods applied in this study. The conclusion to be drawn based on visual inspection of the normality probability plots for all the centroid methods is that, the residuals satisfy the statistic normality assumptions, thus, the residuals are normally distributed. Therefore, since the residuals conform to the normality assumptions, statistic tests on the accuracy measure of the residuals were carried out as shown in table 3 below.

Table 3: Residual Estimation Accuracy Measures

Centroid Method	**Error Term**	**Max(-)/m**	**Max(+)/m**	**Mean Error (m)**	**Standard Error (m)**
Arithmetic Mean Centroid	V_X	-0.152126696	0.173266176	1.66658E-09	0.089595057
	V_Y	-0.918067856	0.709828764	-5.8208E-11	0.464913725
	V_Z	-1.794841314	1.543590025	1.65432E-10	0.837359175
Harmonic Mean Centroid	V_X	-0.149530000	0.174845270	7.35E-10	0.089482389
	V_Y	-0.918080000	0.709861985	-6.13E-12	0.464895038
	V_Z	-1.794670000	1.543759077	1.16E-10	0.837367931
Median Centroid	V_X	-0.152860000	0.173050000	1.23E-09	0.089635933
	V_Y	-0.918060000	0.709790000	-8.12E-11	0.464919065
	V_Z	-1.794880000	1.543550000	4.90E-11	0.837356178
Root Mean Square Centroid	V_X	-0.138700000	0.181980000	7.84E-10	0.089204466
	V_Y	-0.918150000	0.709900000	2.45E-11	0.464798858
	V_Z	-1.793990000	1.544010000	6.74E-11	0.837356774

From the statistical tests of the residuals (V_X, V_Y, V_Z), the maximum negative error, maximum positive error and mean error values given in table 3 above show that, the root mean square and harmonic mean centroid were better than the arithmetic mean and median centroid in both X, Y and Z respectively. However, it was realized that both centroid methods gave negligible values of mean errors. In addition, it can be seen from table 3 above that the horizontal coordinates (X, Y) are much better than the vertical coordinate (Z). This arises from the different horizontal and vertical surveys of the Ghana War Office datum. A careful study of table 3 above shows that the root mean square centroid estimated the 3D coordinates (X, Y, Z) with a significantly better accuracy than the other centroid methods in terms of the standard error. Comparatively, both centroid approaches gave closer accuracies and precision. Thus, the smaller the standard error, the less dispersed are the values in the data set and the more precise is the measurement.

Checking the statistical validity of the derived parameters

A hypothesis test for each of the transformation parameters derived in the computational process was performed at 5% level of significance. This was done to ascertain whether all the values of the parameters determined could be judged statistically different from zero and this confirms their significance. Table 4 below presents the calculated **t** statistic results for the centroid methods.

Testing of Hypothesis: $H_0:\beta_1 = 0$ (Each parameter is not statistically different from zero)

$H_1:\beta_1 \neq 0$ (Each parameter is statistically different from zero)

Significance Level: $\alpha = 0.05$

Test Statistic: $t = \frac{|Parameter|}{SD}$ where SD is the standard deviation of the individual parameters shown in table 1.

Decision Rule: Reject H_0 if $t > t_{(\alpha/2, V),}$ where V is the degree of freedom.

Conclusion: If the calculated t is greater than $t_{\alpha/2,\ V}$, reject the null hypothesis of that parameter and vice versa.

Table 4: Computed t-test values for Centroid Computation Methods

Parameter/ Centroid	t_X	t_Y	t_Z	α	ε	η	S
Arithmetic Mean Centroid	1445.27034	245.22024	2369.37023	280236.69171	12479.83665	2013.44821	4.52875
Harmonic Mean Centroid	1050.24781	207.69005	2024.32406	280046.6965	15642.6523	3219.00531	4.52895
Median Centroid	1410.45373	241.72601	2326.83805	281082.2785	12467.92453	2018.86793	4.53645
Root Mean Square Centroid	259.98526	67.62931	686.43032	279721.519	29371.21212	8582.70677	4.53774

From the student t-distribution tables, $t_{(\alpha/2, V)} = 2.179$. Judging from the ***t*** values obtained (table 4) for the centroid techniques, it can be concluded that all parameters are significantly different from zero at 95% confidence interval, hence, the null hypothesis ($H_0:\beta_1 = 0$) for these parameters were rejected. Therefore, there is a non-zero relationship between the War Office and WGS 84 reference coordinate system. As a result, the conclusion to be drawn here is that, the derived parameters of the centroid procedures applied in this study are all statistically significant.

Test Results Analysis

The effect of systematic model deformations was done by comparing the estimated projected grid coordinates in the War Office system with their corresponding a priori grid

coordinates from another solution in the Ghana Geodetic Reference Network. This creates the opportunity to assess the accuracy and reliability of the transformation parameters determined via Veis model for each of the four centroid techniques applied in this study. To carry out this test, nineteen existing coordinates (check points) were utilized. A summary of the coordinate differences between the projected and existing coordinates within the Ghana Geodetic Reference Network are shown in table 5 below.

Table 5: Summary of coordinate differences test results

Centroid Techniques	Maximum (E)/m	Minimum (E)/m	Maximum (N)/m	Minimum (N)/m
Arithmetic Mean	0.919299020993175	-0.709431121265639	1.02939033906480	-0.876730044754953
Harmonic Mean	0.919285914600246	-0.709498482079634	1.02934705745597	-0.876820570331695
Median	0.919285914600246	-0.709398507702214	1.02944703185113	-0.876720595954275
Root Mean Square	0.919285914600246	-0.709498482079634	1.02904713427048	-0.877513685535695

From table 5 above, it can be seen that the overall accuracy of the centroid techniques are in the order of approximately 0.9 meter and 1.0 meter in the Eastings and Northings which meet the standard accuracy requirement for three-dimensional similarities (Veis model) of 1m. Hence, the centroid techniques horizontal accuracy achieved in this study signifies that, the distortions in the local geodetic network (War Office datum) are at a minimum. However, a careful study of the results obtained for the centroid approaches reveal that, the root mean square centroid method is the preferred technique to be applied in estimating centroid for precise datum parameter determination.

To evaluate the performance and adequacy of the centroid techniques, the coefficient of determination, correlation coefficient and root mean square error were the statistical estimation accuracy measures utilized. These estimation accuracy measures help in assessing the values of the estimation models as well as displaying them graphically. The statistical values (R^2 and r) and the root mean square error (RMSE) values of the test data set's coordinate residuals are presented in table 6 below.

Table 6: Results from statistical test

Centroid Methods		R^2	r	RMSE (m)
Arithmetic Mean	Eastings	1.0	1.0	0.480431700808690
	Northings	1.0	1.0	0.861827906837048
Harmonic Mean	Eastings	1.0	1.0	0.480428049147306
	Northings	1.0	1.0	0.861804169176364
Median	Eastings	1.0	1.0	0.480436159695489
	Northings	1.0	1.0	0.861841180841139
Root Mean Square	Eastings	1.0	1.0	0.480361020886798
	Northings	1.0	1.0	0.861706368517886

In this study, the coefficient of determination (R^2) was used as a criterion to measure the adequacy of the Veis model predictions (projected coordinates) when their related centroid methods estimated parameters were applied to the observations. Based on the results (table 6), the values of R^2 indicated that the centroid procedures describe the variation in the data with highly reliable accuracy. The coefficient of correlation (r) (table 6) corroborated this high strength of linear dependence between the existing and projected coordinates. A sample of the correlation graphs are shown in figure 7 below.

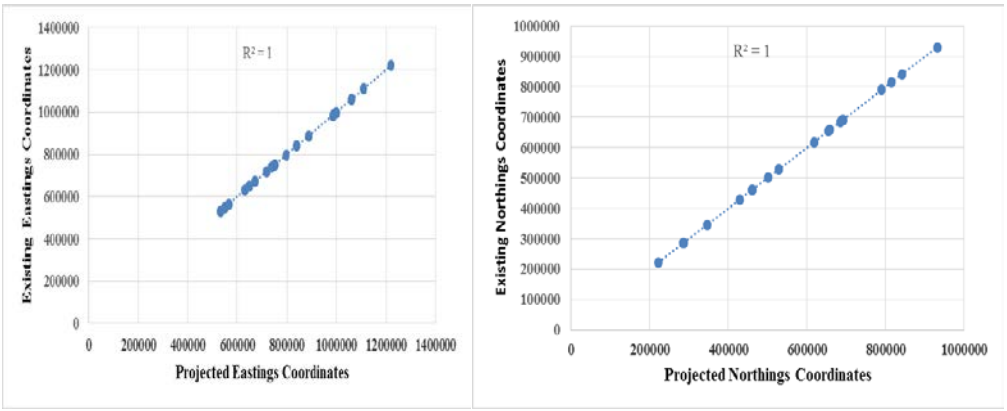

(a) Eastings **(b) Northings**

Figure 7: Scatter plots of existing against projected coordinates for Arithmetic Mean Centroid

To further confirm the degree of correlation between actual and projected coordinates for the centroid strategies, a test of hypotheses (**t** statistic) at 5% significance level was conducted on the correlation coefficients determined.

Testing of Hypothesis:

Null hypothesis: Existing coordinates do not have any correlation with the projected coordinates

$$H_0 : \rho = 0$$

Alternative Hypothesis: Existing coordinates do have correlation with the projected coordinates

$$H_1 : \rho \neq 0$$

Significance Level: $\alpha = 0.05$

Test Statistic:

$$t = r\frac{\sqrt{n-2}}{\sqrt{1-r^2}}$$

Where; r = correlation coefficient (refer to table 9)

n = number of observations = 19

Decision Rule: Reject H_0 if $| t | > t_{\alpha/2, n-2}$

Conclusion: If the calculated $| t |$ is greater than $t_{\alpha/2, n-2}$, reject the null hypothesis and vice versa.

From the student t-distribution tables, $\mathbf{t}_{(0.025, 17)} = 2.110$. A critical observation of the test statistic equation above shows that the test statistic is at infinity because $r^2 = 1$ and therefore the test will be at the tail end of the distribution. Hence, the null hypothesis is rejected because the calculated **t** is greater than the critical value; this makes it highly significant. This further confirms that the results established a strong correlation between the existing and projected coordinates.

The RMSEs shown in table 6 above, were used in the evaluation process because the RMSEs are sensitive to even small errors and can determine the quality of a transformation, making it good in comparing small changes between projected and observed differences in models. From table 6 above, it is evident that the root mean square centroid estimated the smallest RMSEs for 2D coordinates (E, N) of the test points with a significantly better accuracy than the other centroidal techniques. In addition, the arithmetic mean, harmonic mean and median centroid produced identical results of RMSE values. This confirms the assertion that there is no much significant difference between the centroid computational methodologies.

Figure 8 below, is a root mean squared error distribution in both Eastings and Northings for the centroid approaches. This distribution shows the accuracy of the centroid methods estimations for a set of test data and determines how well the estimation performed. The bar chart shows the root mean square error distribution and the bar height represents the root mean square of the difference between the existing coordinates that fall within the range of the bin and their projected coordinate values. Moreover, by comparing the RMSE values to the achievable accuracy standard for the centroid methods, it can be stated that the transformation results are within tolerance.

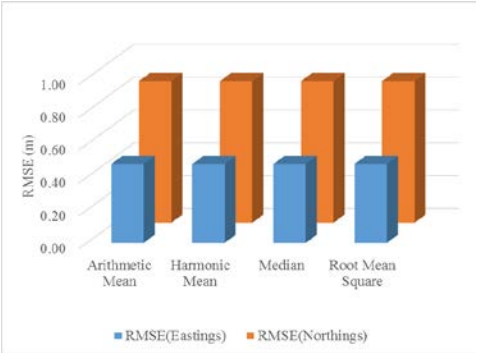

Figure 8: A graph of RMSE in Eastings and Northings for the Centroidal Methods

Visual observation of figure 8 shows that the estimations in Northings coordinates gave a lower accuracy compared to the Eastings. This may perhaps be attributed to the effect of the height determined for the Ghana War Office ellipsoid when the iterative abridged Molodensky was used to estimate change in ellipsoidal height since there is no existence of geoid in Ghana. Thus, the geoid undulation could not be determined. Therefore, applying the Bowring Inverse equation in estimating the latitude will incur some errors that will affect the final projected coordinates in Northings. However, the projected Eastings coordinates of the Ghana War Office system were better because the computation of the longitude uses the horizontal coordinates (X, Y) which are determined to a better accuracy.

Software Designed Interface

An executable program (figure 9 below) using MFC AppWizard (exe) in Microsoft Visual Studio 2005 was designed for the Bowring's forward equation for converting geodetic data into rectangular cartesian coordinates. The purpose of designing this software was by the fact that, the coordinate conversion as described in the methodology is the fundamental step that is needed to be carried out in any GPS coordinate transformation parameters determination. Also, literature and researches related to this area of work in Ghana have shown that there is no existence of such software. Therefore, this software designed will serve as a preliminary concept and create awareness for future modifications and development for geospatial and non-geospatial communities in Ghana. The designed interface (figure 9 below) can be used by inputting geodetic coordinates of common points between the two systems and clicking on the calculate bottom to estimate the corresponding 3D cartesian coordinates.

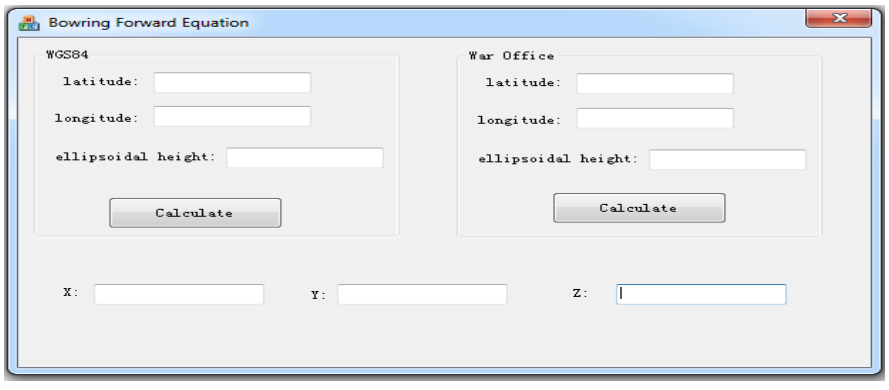

Figure 11: The designed Interface

Conclusion

Four sets of centroid computational methods namely; arithmetic mean, harmonic mean, median and root mean square have been investigated. The analyses conducted in this study

show that the transformation parameters of root mean square centroid are more realistic than those of arithmetic mean, harmonic mean and median centroid. That is, in order to obtain precise GPS transformation parameters the root mean square is the most appropriate method to be applied to estimate the centroid coordinate system. It is worth mentioning that GPS coordinate transformation parameters determined for any geodetic application is used by geospatial and non-geospatial professionals for various purposes. For this reason, in order to facilitate setting a standard in practice, the root mean square centroid over the other centroid methods is proposed to be used, especially in transformations within local geodetic networks.

Acknowledgement

The author is highly indebted to China University of Geosciences (Wuhan) and Ghana Survey Department for their support.

References:

Anon, Ghana from: http://en.wikipedia.org/wiki/Ghana. Accessed on: 4th May, 2013.

Ayer, J. and Tiennah, T. Datum Transformation by the Iterative Solution of the Abridging Inverse Molodensky Formulae. The Ghana surveyor, Vol. 1, no. 2, pp. 59-66, 2008.

Baabereyir, A. Urban environmental problems in Ghana: case study of social and environmental injustice in solid waste management in Accra and Sekondi-Takoradi. Thesis submitted to the Department of Geography, University of Nottingham for the Degree of Doctor of Philosophy, UK, 2009.

Constantin-Octavian, A. 3D Affine coordinate transformations. Masters of Science Thesis in Geodesy No. 3091 TRITA-GIT EX 06-004, School of Architecture and the Built Environment, Royal Institute of Technology (KTH), 100 44 Stockholm, Sweden, 2006.

Dzidefo, A. Determination of Transformation Parameters between the World Geodetic System 1984 and the Ghana Geodetic Network. Masters Thesis, Department of Civil and Geomatic Engineering, Kwame Nkrumah University of Science and Technology, Kumasi, Ghana, 2011.

Deakin, R.E. The standard and Abridged Molodensky Coordinate Transformation Formulae Department of Mathematical and Geospatial Sciences, RMIT University pp.1-21, 2004.

Deakin, R.E. A Note on the Bursa-Wolf and Molodensky-Badekas Transformations. School of Mathematical and Geospatial Sciences, RMIT University pp.1-21, 2006.

Deakin, R.E. Coordinate Transformations for Cadstral Surveying. School of Mathematical and Geospatial Sciences, RMIT University pp.1-33, 2007.

Featherstone, W. and Vanicek, P. The Role of Coordinate Systems, Coordinates and Heights in Horizontal Datum Transformations. The Australian Surveyor, Vol. 44, No. 42, p.143-149, 1999.

Hofmann-Wellenhof, B., Lichtenegger, H., and Collins, J. GPS Theory and Practice. 4th edition, Springer-Verlag, Wien, New York, 1997.

Kutoglu, S.H., Mekik, C. and Akcin, H. A Comparison of Two Well Known Models for 7-Parameter Transformation. The Australian Surveyor, Vol.47, No.1, 1pp, 2002.

Leick, A. and Gelder, B.H.W. On the similarity transformations and geodetic network distortions based on Doppler satellite observations. Reports of the department of Geodetic Science, Report No.235, Ohio State University, Columbus, Ohio, USA, 1975.

Marzooqi, Y. Al., Fashir, H., and Syed I.A. Derivation of Datum Parameters for Dubai Emirates. FIG. Working Week, 2005 and GSDI-8. Cairo, Egypt. April 16-21, pp. 2-10, 2005.

Newsome, G.G. and Harvey, R.B. GPS Coordinate Transformation Parameters for Jamaica. Survey Review, Volume 37, Number 289, pp:218-234 (17), 2003.

OGP Publication 373-7-2 – Geomatics Guidance Note number 7, part 2 – July 2012, 89 pp.

Poku-Gyamfi, Y. and Schueler, T. Renewal of Ghana's Geodetic Reference Network 13th FIG Symposium on Deformation Measurement and Analysis, 4th IAG Symposium on Geodesy for Geotechnical and Structural Engineering, LNEC, LISBON, pp.1-9, 2008.

Rapp, R.H. Geometric Geodesy - Part II, Department of Geodetic Science and Surveying, The Ohio State University, pp. 68-72, 1993.

Thomson, D.B. A study of the Combination of Terrestrial and Satellite Geodetic Networks. Doctorial Thesis, Department of Surveying Engineering, University of New Brunswick, Canada, pp. 89-128, 1994.

Yao Yevenyo Ziggah, Hu Youjian and Christian Odutola Amans. Determination of GPS Coordinate Transformation Parameters of Geodetic Data between reference datums - A Case Study of Ghana Geodetic Reference Network. International Journal of Engineering Sciences and Research Technology, Vol. 2 Issue 4, 2013.